First-principles studies of lithium adsorption and diffusion on silicene with grain boundaries

Xiao Wang,[1] Huazhong Liu,[2] Marko Huttula,[3] Youhua Luo,[1] Meng Zhang,[1,*] Wei Cao[3,*]

[1] *Department of Physics, School of Science, East China University of Science and Technology, Shanghai 200237, China*

[2] *Department of Basic Courses, Wuhan Donghu University, Wuhan, 430212, China*

[3] *Nano and Molecular Systems Research Unit, University of Oulu, P.O. Box 3000, FIN-90014, Finland*

Correspondence to: Meng Zhang (Email: mzhang@ecust.edu.cn) and Wei Cao (Email: wei.cao@oulu.fi)

Abstract

As a close relative to graphene, silicene is advanced in high lithium capacity, yet attracting various manipulation strategies to promote its role in energy storage. Following grain boundary (GB) engineering route as widely used in graphene studies, in this work, first-principles calculations were performed to investigate adsorption and diffusion behaviors of lithium on silicene with GBs of 4|8 or 5|5|8 defects. In both GB forms, donation of the Li 2s electron to the GBs significantly increases the Li adsorption energy, while small energy barriers facilitate the Li migration on the silicene surface. Furthermore, the large hole of GB (4-8) also permits easy penetration of the Li ions through the defective silicene sieve. These important features demonstrate GBs are beneficial for enhancing capacity and charge speed of the Li batteries. Thus, superior anodes made of silicene with GBs are expected to serve a key solution for future energy storages.

1. INTRODUCTION

The rechargeable lithium ion batteries (LIBs) are the predominant energy reservoirs in electric vehicles and portable electronics. However, future batteries require smaller LIB dimensions, lighter weights, along with higher energy densities. To meet these stringent requirements, extensive researches have been emphasized on explorations of the advanced electrode materials which can provide high charge capacity, long cyclic stability, high-rate capability and safety.[1-3] Graphene and oxidized graphene have been found with higher capacities of 600 to 1000 mAh/g[4,5] than the bulk counterpart of graphite (372 mAh/g).[6] In analogy to these organic monolayers, other two-dimensional (2D) materials were also studied and considered as important candidates for the LIBs anodes. So far, explorations have been searched within naturally occurring species as graphdiyne,[7] molybdenum disulfide (MoS_2)[8] and boron carbon nitride nanosheets,[9] etc.

The synthetic monolayers may also act as anode materials for Li storage. Recently, silicene - the silicon monolayer, has been synthesized on various metal substrates such as Ag, Ir and ZrB_2.[10-13] Preliminary results have shown that high Li capacity is feasible on nanostructured silicon (e.g. silicon nanowires,[14,15] nanoparticles[16]) but with small volume deformations of the matrices. Thus, silicene is also expected to be a good candidate for LIB electrodes because of its nature of low-dimensional silicon and structural similarity to graphene. In fact, theoretical studies have indicated that the binding energy between Li and silicene is 2.2 eV per Li atom and the barriers for Li diffusion are less than 0.6 eV,[17,18] much lower than that

of Li diffusion on graphene.[19,20] Moreover, silicene is exempt from irreversible structural changes during lithiation/delithiation processes in comparison with crystalline silicon.[21] Thus, silicene may act as an alternative of graphene on the LIB electrodes.

However, the unavoidable defects associated with material synthesis bring substantial impacts, either beneficial or detrimental, on the physical, chemical and electronic properties of the low dimensional materials.[22,23] Several works have been concentrated on the structural and electronic properties of point defects in free-standing silicene.[24-27] Another important kind of structurally robust defect is topological line defects (LDs), which remain stable against local geometrical rearrangements.[28,29] Different types of line defects are already found at the grain boundaries (GBs) of graphene,[30,31] hexagonal boron nitride,[32] molybdenum disulphide,[33] etc. As for silicene, several types of GBs have been identified during the growth on Ag(111) via molecular-beam epitaxy technique.[26] A large number of defect clusters were also observed in the scanning tunneling microscope (STM) images of silicene, where more than three Si vacancies compose the extended line defects.[34] Moreover, the STM result showed that patterned defect structures behave as vacancies, pentagon-heptagon pairs, square-octagon pairs on single-layer silica films on Ru(0001).[35] Furthermore, in the graphene studies, introducing GBs will enhance the capacity of Li (or Na) adatoms and lower energy barriers of the diffusions of these adatoms along the GBs. Thus, graphene with GBs are considered beneficial for the LIBs or sodium ion batteries (NIBs).[36,37]

Despite dedications in materials synthesis and property studies, the role of GBs remains elusive for the adsorption and diffusion of lithium on silicene. A key question arises that if such GB defects will be beneficial as the case of graphene, or introduce shrinkage of the battery capacity. In this work, we present a systematic computational investigation of the adsorption behavior of Li on silicene with GBs. The surface diffusion and diffusion through silicene were also studied to evaluate the energy barriers that affect the charging rates and cyclic performance. To the best of our knowledge, it is the first time to apply the GB engineering for silicene in energy researches.

2. COMPUTATIONAL METHOD

The computations are carried out using unrestricted spin-polarized DFT, implemented in the Dmol3 code.[38-40] A PerdewBurkeErnzerhof (PBE) functional of generalized-gradient approximation (GGA) is used for calculating exchange correlation functions.[41] The double numerical plus polarization function (DNP) is chosen as the atomic orbital basis set.[40] The dispersion corrections of Tkatchenko-Scheffler[42] are adopted to describe the van der Waals interactions in our systems. A k-points grid sampling equivalent[43] 10 × 10 × 1 in the unitary cell is considered. A basis set cutoff of 4.6 Å is employed for all systems, and the effect of periodic boundaries is negligible. All atoms are allowed to relax until the forces on each atom are smaller than 0.001 Ha/ Å, with the convergence threshold energy of

10^{-6} Ha.

Two kinds of grain boundaries are considered. The first one is the 4|8 defect along the armchair boundary (GB(4-8)) and the second the 5|5|8 defect along the zigzag chain (GB(5-8)). We simulated 2D sheets by employing periodic boundary conditions. A vacuum of 20 Å is used to avoid the interactions between periodic images. The relative stability of the LD defect comparing with freestanding silicene can be estimated by the formation energy, E_f, which is defined as

$$E_f = [E_{GB} - E_P]/L$$

where E_{GB} and E_P are the total energies of the defective and pristine silicene, respectively, and L represents length of the grain boundary.

Four typical adsorption sites are considered as the possible adsorption sites on pristine silicene, including the hollow (H) site above the center of a hexagon ring, the site on the top of Si atom in higher plane (T), the site on the top of the Si atom in lower plane (V) and the bridge (B) site above the midpoint of a Si-Si bond. Based on our previous results of Li adsorption on non-defective matrix,[21] we considered two types of adsorption sites on the defected silicene: the H site above the center of a polygon (four-membered, pentagon, or octagon) ring and T site on the top of Si atoms in higher plane around the defective region. The adsorption energy (E_{ads}) of Li is obtained as

$$E_{ads} = E(total) - E(sheet) - E(Li)$$

where E(total), E(sheet), and E(Li) are the total energies of relaxed silicene with Li

adsorption, the isolated silicene sheet and the isolated Li atom. According to the definition, negative adsorption energy denotes an energetically favorable Li adsorption to silicene.

To study the effect of grain boundaries on the diffusion of Li on silicene, the energy barrier ΔE of Li diffusion is calculated. Linear synchronous transit (LST) with the quadratic synchronous transit (QST) method was used to search for minimum energy path.[44] Then the transition state was confirmed by the nudged elastic band (NEB) method.[45]

3. RESULTS AND DISCUSSIONS

3.1 GBs in silicene monolayer

The GB(4-8) in silicene is formed along the armchair edges as shown in Figure 1. After full relaxation, the neighboring half-lattices couple to each other and form periodic arrays of octagonal and four-membered rings. The GB(5-8) contains two pentagons spatially separated by an octagonal ring, following the removal of silicon dimmer stilted 30º from the zigzag chain. The formation energies for GB(4-8) and GB(5-8) structures are 0.20 eV/Å and 0.15 eV/Å, respectively. These results suggest that the formation of GBs in a silicene sheet is easier compared with its counterpart in graphene. And the GB(5-8) is more energetically favorable than GB(4-8), in agreement with previous calculation.[46]

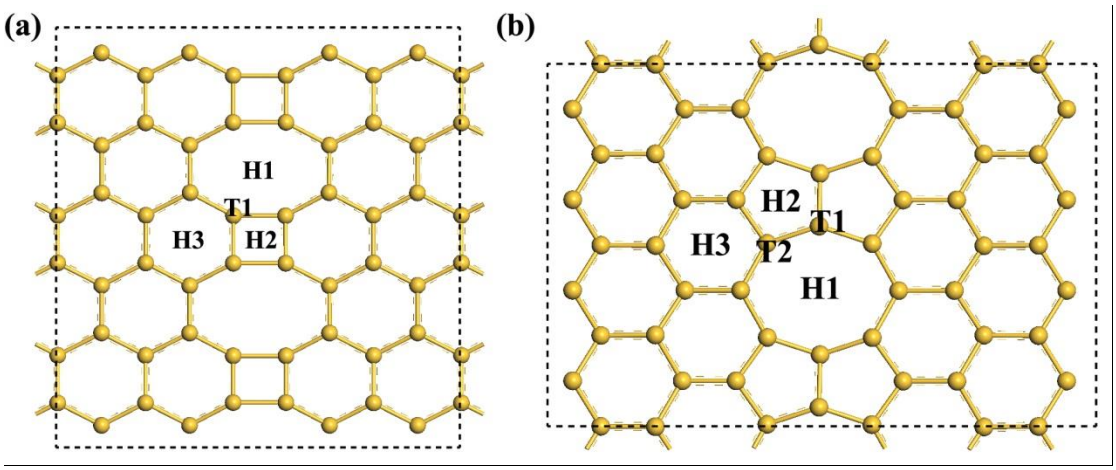

FIGURE 1 Optimized atomic structures of silicene with (a) 4|8 and (b) 5|5|8 GBs. The considered sites for adsorption of a Li atom are indicated by the black labels.

3.2 Adsorption of Li on silicene monolayer with GBs

In the case of Li adsorption on perfect silicene, a hollow site with one Li ion is the lowest energy configuration with adsorption energy of -2.41 eV according to our previous study.[21] The metal adatom drift over to an H site when placed above a B site.

For Li adsorption on GB(4-8) sheet, considering the symmetry, various adsorption sites are examined including Li adsorption on the hollow site of polygonal rings and at the top of Si atoms round the defective region as shown in Figure 1. All the adsorption energies of stable configurations are summarized in Table 1. It is found that the most stable site for Li adsorption is the hollow site of the octagonal ring (H1) (Figure 2). The E_{ads} is 0.47 eV lower than the adsorption energy on the hollow site of perfect silicene. The distance (d_{Li-Si}) of the adsorbed Li atom and silicene surface is

0.912 Å, which is also much shorter than the non-defective case due to its larger adsorption energy. In addition, for Li adsorbed on different sites above GB(4-8), the stability of Li adatom from high to low exhibits the following order: octagonal ring > hexagonal ring > four-membered ring > the top of Si atom.

TABLE 1 The stable configurations of Li adsorption on defective silicene sheets and their adsorption energies (E_{ads}).

Li adsorption on GB(4-8)		Li adsorption on GB(5-8)	
Model	E_{ads} (eV)	Model	E_{ads} (eV)
H1	-2.88	H1	-2.74
H2	-2.61	H2	-3.09
H3	-2.81	H3	-2.85
T1	-2.58	T1	-2.88
		T2	-2.84

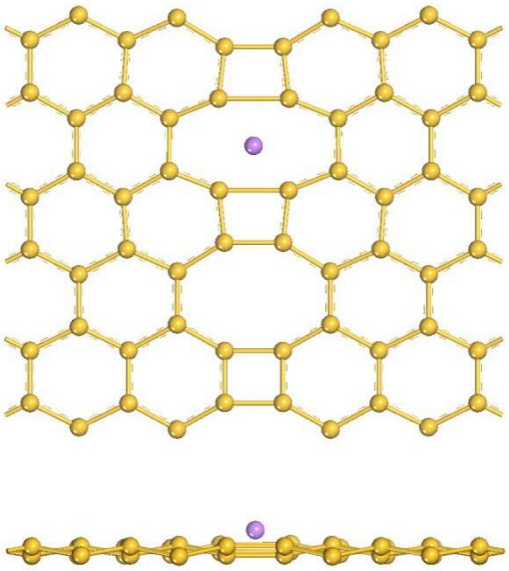

FIGURE 2 Optimized structure for Li adsorbed in the plane of an octagonal ring of GB(4-8): (a) top view and (b) side view.

For the GB(5-8) structure, various adsorption sites were considered as shown in Figure 1. It is found that the H2 site (see Table 1 and Figure 3) is the most stable one for Li adsorption with an E_{ads} of -3.09 eV. For the different hollow sites above the polygonal rings of GB(5-8), the stability of a Li adatom from high to low exhibits the following order: pentagonal ring > hexagonal ring > octagonal ring. It is reversed as compared with the case of GB(4-8), in which octagonal ring is the most stable site for Li adsorption, suggesting the adsorption of Li in silicene depends on the kinds of grain boundaries. In addition, Li adsorbed at the top of Si atoms exhibits higher stability than on octagonal ring. Similar to the case of GB(4-8), Li adatom energetically prefers the sites around the defect region to those at non-defective region. The interaction of Li adatom and GB(5-8) is stronger than that of Li adatom and

GB(4-8). Negative adsorption energies for a range of adsorption sites indicate that Li storage over silicene with GBs is a spontaneous process. Generally speaking, Li clusters may form with increasing the Li content. The formation of Li cluster would reduce the charge ability of LIBs and induce dendrite growth of lithium, which is harmful to battery safeties. Thus, we also investigated Li dimer adsorption on the defective systems. A Li dimer is firstly placed on silicene assumed that the hollow site is energetically favorable for each Li atoms and both Li atoms contact with the silicene surface. After optimization, structural changes can be clearly observed in Figure 4. The bond length of Li dimer is largely increased and the dimer cannot keep its configuration. Finally, two Li atoms from the dimer are separately adsorbed on the different hollow centers of GB(4-8) or GB(5-8) with average adsorption energies of -2.77 eV/atom or -2.74 eV/atom. The absolute values of these energies are smaller than those from single Li atom adsorption cases as shown in Table 1, but much larger than the cohesive energy of bulk bcc lithium (-1.68 eV/atom).[47,48] The results indicate that the existence of GBs could prevent the formation of Li clusters on silicene and suggest that Li atoms prefer adsorption on silicene with GBs.

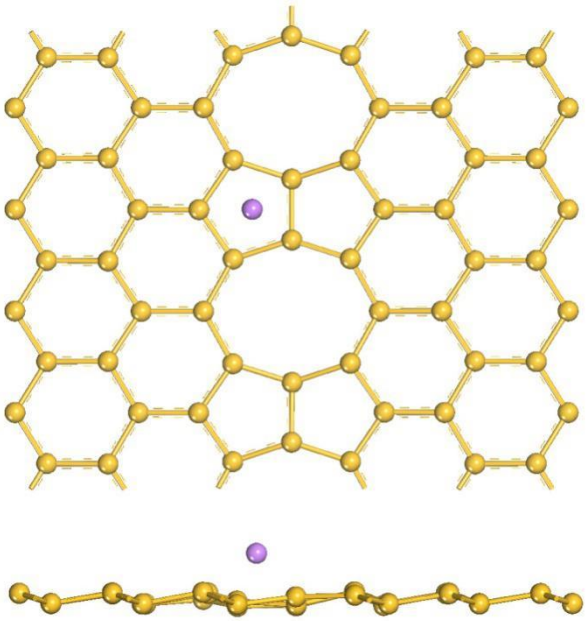

FIGURE 3 Optimized structure for Li adsorbed at the top of H2 site of GB(5-8): (a) top view and (b) side view.

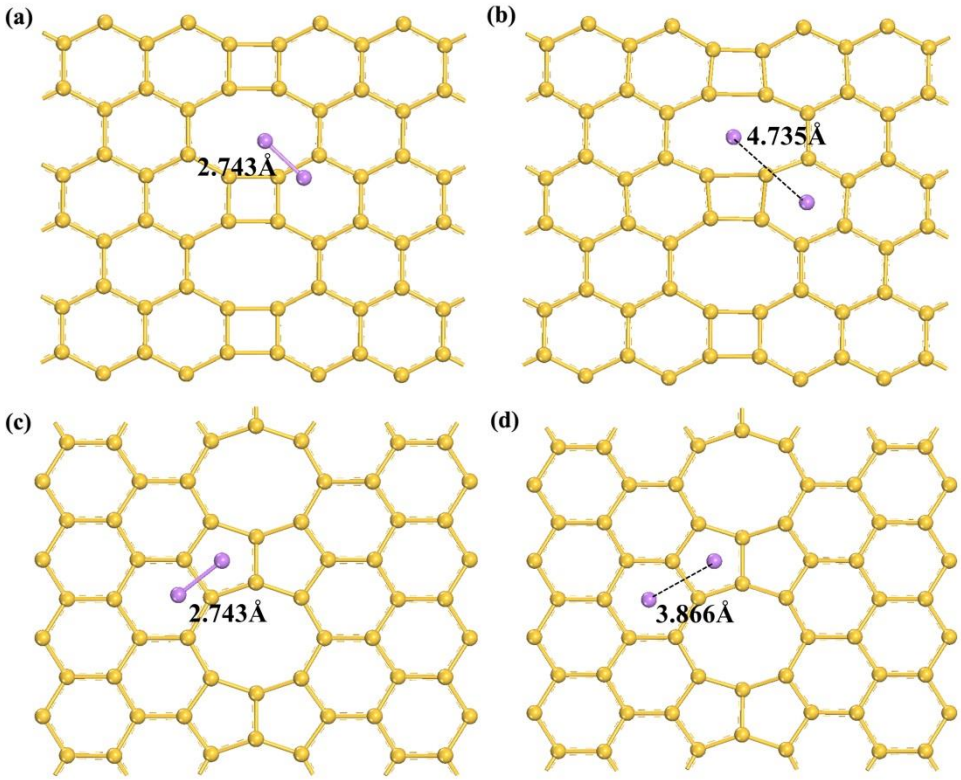

FIGURE 4 (a) and (c) are configurations that Li dimer adsorbs on GB(4-8) or GB (5-8) before optimization, (b) and (d) are that after optimization.

3.3 Electronic properties of silicene with Li adsorption

To analyze the nature of Li-silicene interaction, we compute the electronic structures of silicene with the adsorbed Li. The projected density of states (PDOS) of the GB(4-8) with Li adsorption in Figure 5 show that after Li adsorption, the valence states of the system consist mainly of 3p states of Si atoms and 2p states of Li. The strong hybridization between the p orbitals of Li and the four Si atoms denotes the typical feature of chemical adsorption. Figure 6 presents the deformation charge density of this system. Obviously, strong combined ionic and covalent Li-Si bonds are formed after adsorption as reflected in the length of the Si-Si bonds around the Li atom elongating about 20% and consequently swelling the octagonal Si ring. The charge accumulation takes place near the puckered octagonal ring of GB(4-8) while charge-depleted regions surround the Li atom, indicating net charge transfer from the metal adatom to silicene. The Hirsheld charge analysis results further show that the charge transfer mainly occurs between the nearest up- and down-Si atoms in octagonal ring and Li atom. With the charge transferring, Li atom injects 0.12 e into the antibonding orbitals of these reactive Si atoms. The strong hybridization between Li and Si as well as the notable charge transfer verify that the strong Si-Li interaction exists in silicene with GBs and results in the high stability of the structure.

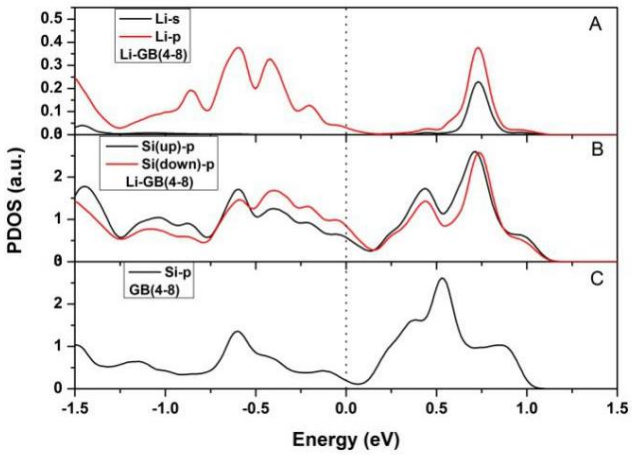

FIGURE 5 Density of states for the GB(4-8) with and without Li adsorption. A and B are the PDOS of the adatom Li and the defective region of Si atoms in Li adsorbed GB(4-8). Si(up) represent the nearest Si atoms above Li atom in Figure 2, and Si(down) mean the nearest Si atoms below Li atom. For comparison, C is the DOS of the Si atoms in GB site in GB(4-8) without Li adsorption.

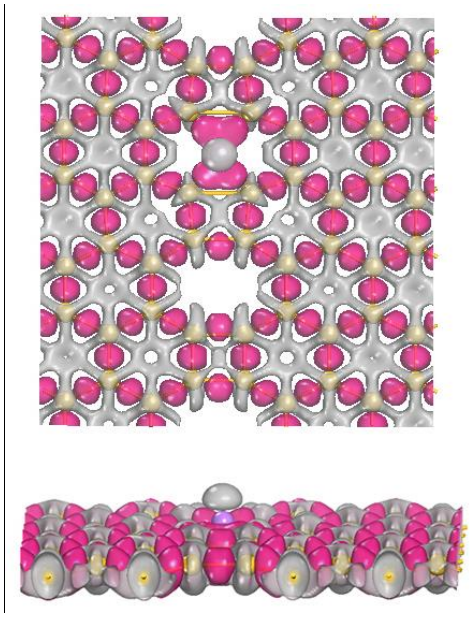

FIGURE 6 Top view and side view of deformation charge density plots for the most stable adsorption sites for Li over GB(4-8). Red and grey regions indicate charge accumulation and depletion, respectively.

The bonding mechanism of Li atom adsorption on GB(5-8) is also presented in Figure 7. Detailed studies of DOS show that the p states of Li atoms hybridize with p states of Si atom in pentagon ring with a wide broadening which illustrates that the interactions between Li atom and GB(5-8) is also a strong chemical adsorption, similar to Li with GB(4-8). The wider energy states broadening suggests a stronger hybridization between pentagon ring and Li atom. According to Hirsheld analysis, Li atom transfers 0.25 e into GB(5-8). The larger charge transfer shows a stronger adsorption, in agreement with the PDOS analysis. However, with the electrons transfer into the bonding orbitals of pentagon ring, the Si-Si bonds of pentagon ring is subjected to very small changes (with the elongation of about ~1%), implying the stability of pentagon ring defect is larger than the octagonal ring defect. This is reasonable since the octagonal ring has a more loose geometric structure than the pentagon ring. It is also worth noting that line defects can significantly modify the electronic properties of silicene which transform semimetallic silicene into metallic. After Li adsorption, the metallic characteristic of both GB(4-8) and GB(5-8) remain.

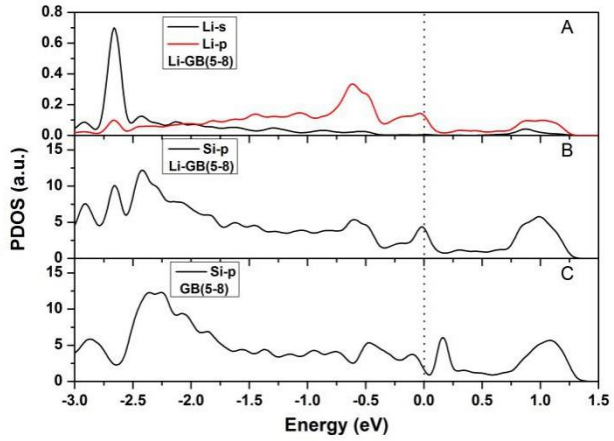

FIGURE 7 Density of states for the GB(5-8) with and without Li adsorption. A and B are the PDOS of the adatom Li and the defective region of Si atoms in Li adsorbed GB(5-8). For comparison, C is the DOS of the Si atoms in GB site in GB(5-8) without Li adsorption.

3.4 Diffusion of a Li adatom on silicene

As the charging rate of the LIBs relies on the Li ion mobility in the anode material, we further studied the Li diffusion on the silicene monolayer with GBs. When Li adatom diffuses on a perfect silicene, it is known that the Li atom would move from a hollow site to a nearest neighboring one by passing the top of Si atoms with an energy barrier of about 0.27 eV. For the diffusion of a Li atom on the silicene with GBs, we consider two types of diffusion paths, namely, the migration along and perpendicular to the GB. The calculated energy profiles for the Li atom diffusion between two neighboring sites on the GB(4-8) (H1 to H2 and H1 to H3) are indicated in Figure 8 and the detailed results are listed in Table 2. Similar to the diffusion on the pristine matrix, the paths between two hollow sites are curves bent

towards a silicon atom. 0.26 eV is needed for lithium to diffuse out of the octagonal ring. Although the Li adatom may be trapped at the hollow site above the octagonal ring of GB(4-8) with larger adsorption energy, the trap will not obviously influence the diffusion energy of Li on the surface of silicene. Then the energy barrier for Li moving into the four-membered ring or the hexagonal ring is 0.03 eV or 0.08 eV, respectively, suggesting a tendency of Li diffusion along the boundary. In addition, the energy barriers for the forward diffusion of a Li adatom are larger than those of the backward diffusion. As a result, the Li adatom tends to diffuse toward the octagonal ring site along the boundary.

Two diffusion paths were considered for the Li diffusion on GB(5-8) (H2 to H1 and H2 to H3), and the energy curves as a function of relative diffusion coordinates are shown in Figure 9. The energy barrier is 0.19 eV and 0.22 eV for Li diffusing from position H2 to T1 and T2, respectively. Compared with Li diffusion on the GB(4-8), Li adatom prefers to diffuse perpendicular to boundary in GB(5-8). The total energy barrier of Li moving from H2 to H3 decreases about 0.14 eV compared with the value of Li diffusion along the boundary. It is noted from Table 2 that the diffusion barriers for backward diffusion were largely reduced, therefore, the Li atom also tends to diffuse to the defective pentagon. The maximum diffusion barriers are 0.16 and 0.10 eV for backward diffusion of Li atoms from H1 or H3 site to H2, respectively. From these results, we can conclude that the GBs not only enhance the adsorption of Li, but also affect the Li diffusion behavior on silicene, especially for the backward diffusion.

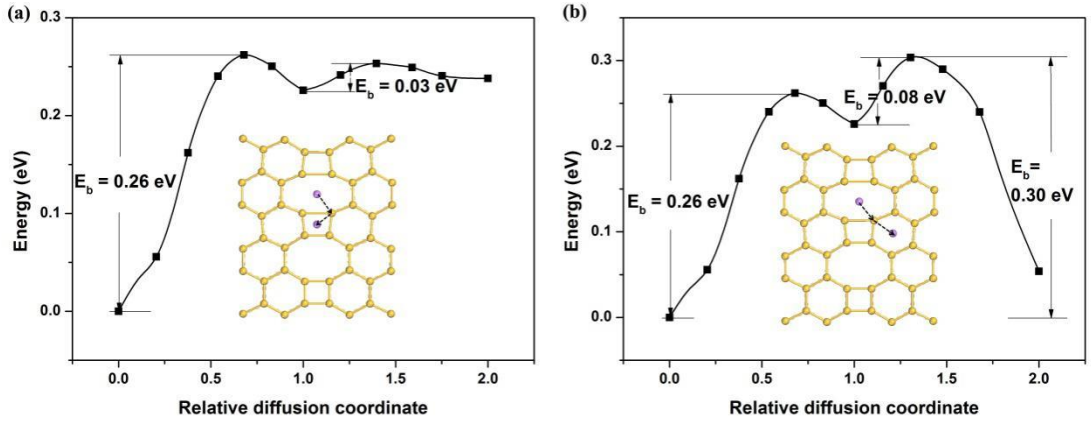

FIGURE 8 Energy curves for Li ion diffusion on silicene with 4|8 GB following the path of (a) H1 to H2 and (b) H1 to H3.

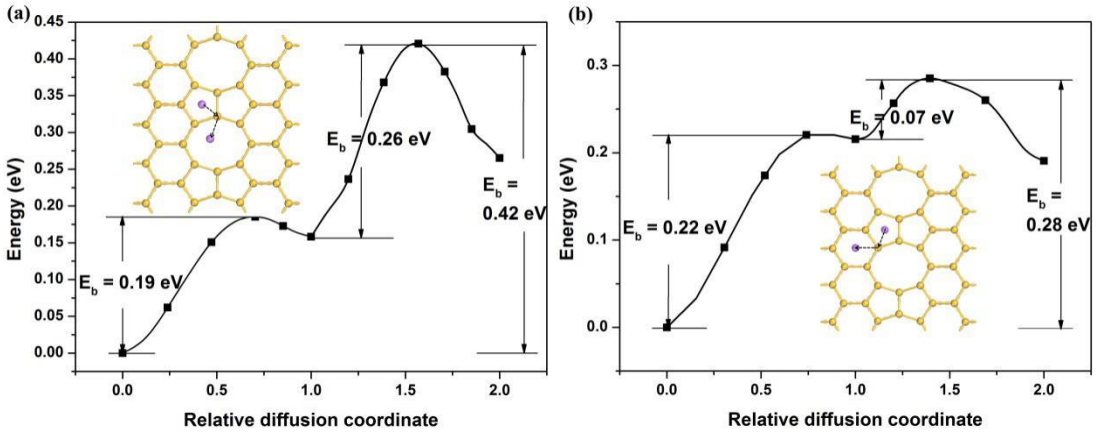

FIGURE 9 Energy curves for Li ion diffusion on silicene with 5|5|8 GB following the path of (a) H2 to H1 and (b) H2 to H3.

TABLE 2 Energy barriers (E_b, in eV) for the diffusion of Li on silicene with 4|8 and 5|5|8 GBs.

System	along boundary		perpendicular to boundary		Through the plane
GB(4-8)	H1 → T1	T1 → H2	H1 → T1	T1 → H3	octagon
E_b (eV)	0.26 (0.04)	0.03 (0.02)	0.26 (0.04)	0.08 (0.25)	0.04
GB(5-8)	H2 → T1	T1 → H1	H2 → T2	T2 → H3	pentagon
E_b (eV)	0.19 (0.03)	0.26 (0.16)	0.22 (0.01)	0.07 (0.10)	2.92

*The values in the parentheses correspond to the energy barrier of a backward diffusion.

3.5 Migration of Li through silicene monolayer with GBs

The diffusion of Li through the defects is also worthy exploring because 2D materials would likely be stacked in layers as the surface-to-volume ratio is higher than having only a single sheet.[49,50] Additionally, ion orientations on double-sided monolayers show exceptional properties due to geometrical arrangements.[51] Previous studies have shown that it is difficult for Li ions to get through from one side of graphene to the other side because of the large energy barriers.[19,52] To compare silicene with graphene, we investigated the diffusion barriers through the sheet and our value for pristine silicene is 1.37 eV, which is much smaller than that of Li

through the graphene. This is because the area of the hollow site of graphene is smaller than that of silicene. The larger area for silicene makes it easier for lithium to get through. Table 2 and Figure 10 clearly denote free diffusion of Li from one side to another side of the silicene plane with the 4|8 GB. As a result of the hollow structure, diffusing through the center of octagonal ring requires only 0.04 eV, which suggests lithium atoms can pass through the hollow site with a high probability.

The mechanism of Li penetration to the defective silicene is also studied. When Li adsorbs on silicene, it possesses a positive charge after donating 2s electron. The extra charge transferred from Li mostly stays at Si atoms near the Li atom, hence, the interactions between them can be ascribed to the coulomb interaction. The octagonal ring in GB(4-8) provides a large open space for Li penetration. This gives electrostatic charge overlapping minimized and a large bond length of 2.552 Å at the barrier state could be found as shown in Figure 11(a), larger than the bond length of 2.369 Å for the Li-Si dimer. Thus, steric hindrance is minimized. The charge difference between the adsorption and the barrier states is 0.03 e. These factors induced a very small diffusion barrier height 0.04 eV.

Since the Li atom prefers to adsorb on the defective pentagon in the case of GB(5-8), it is also worthy to investigate diffusion behavior of Li through the hole. However, a penetration energy of 2.92 eV was calculated, even larger than the value of the Li diffusion through the hexagonal hole in a perfect silicene. As the Li approaches to the barrier site, the available space for Li is narrow with a short separation distance of 1.903 Å, invoking severe charge overlapping between Li and

adjacent silicon atoms. This increases repulsive forces, giving rise to large diffusion barrier height. Thus, among the studied cases, the GB of 4|8 serves best diffusion channels for the Li via diffusions through the octagonal ring and then freely go through it to another surface or the surface of other silicene layer for silicene-based nanostructures.

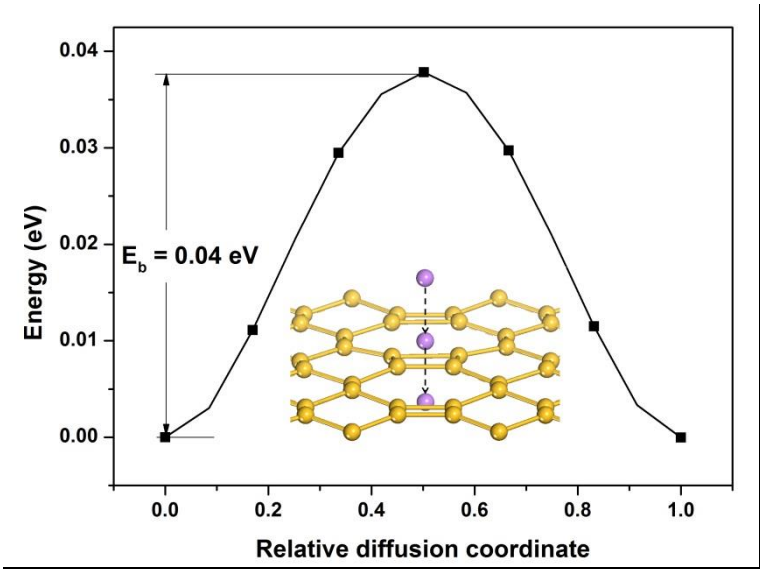

FIGURE 10 Energy curves for Li diffusion in the direction perpendicular to GB(4-8).

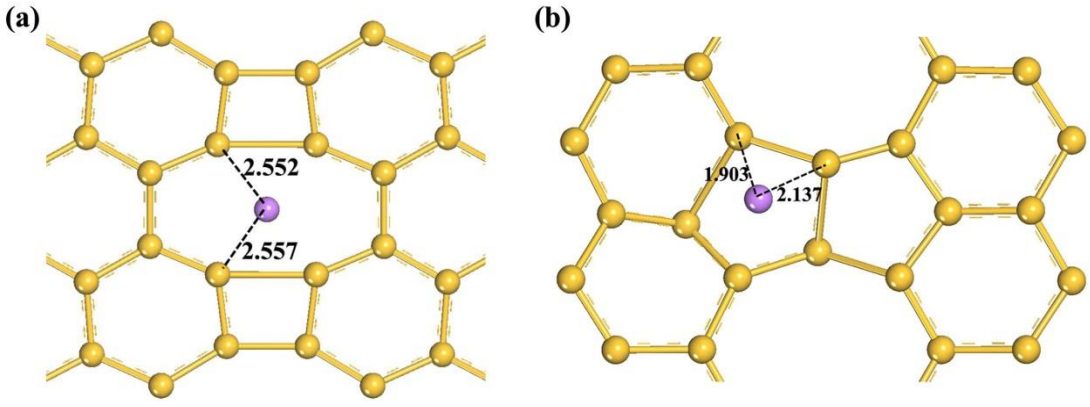

FIGURE 11 The bond lengths (in Å) of Li through silicene (a) with GB(4-8) and (b) with (5-8) at the barrier states.

4. CONCLUSIONS

In summary, based on density functional theory calculations, we have investigated adsorption and diffusion behavior of lithium atoms on silicene with 4|8 and 5|5|8 grain boundaries. Our results show that Li is more strongly bounded to silicene with GBs compared with perfect ones. The donation of Li 2s electron to the defects causes a strong interaction, thus enhances the adsorption. Moreover, diffusion of lithium atoms across and through the substrate is also an important consideration in the cycle performance of LIBs. It is found both GBs cases could significantly facilitate the diffusion behavior of the Li adatoms. Furthermore, the small energy barrier of Li atom enables rather easy penetration of the Li through the sheet of GB(4-8), suggesting the usages of the defective silicene as the sieve for Li atoms during the charge and discharge processes of LIBs. Due to these important features of the GB defective silicene, the present work is hoped to enlighten experimental realizations of the novel anodes for LIBs, and applications for the future energy resources eventually.

AUTHOR CONTRIBUTIONS

The work was conceptualized, investigated and originally drafted by X. Wang., under a general supervision by M. Zhang. X. Wang and W. Cao curated the data interpretation with helps from H. Z. Liu and M. Huttula. Project administrations were performed by Y. H. Luo and M. Huttula. All authors reviewed, edited, and approved

the manuscript.

FUNDING INFORMATION

National Science Foundation of China, Grant/Award Number: 21303054; Fundamental Research Funds for the Central Universities, Grant/Award Numbers: 222201714050, 222201714018; Profile Funding of Academy of Finland, Grant/Award Number: 311934.

RESEARCH RESOURCES

All the computation simulation was undertaken with the resources provided from the High Performance Computing Center of East China University of Science and Technology.

Keywords:

Lithium adsorption and diffusion, first-principles simulations, silicene, grain boundary

REFERENCES

[1] G. L. Soloveichik, *Annu. Rev. Chem. Biomol. Enq.* **2011**, *2*, 503.

[2] J. Liu, *Adv. Funct. Mater.* **2013**, *23*, 924.

[3] H. Pauna, X. Y. Shi, M. Huttula, E. Kokkonen, T. H. Li, Y. H. Luo, J. Lappalainen, M. Zhang, W. Cao, *Appl. Phys. Lett.* **2017**, *111*, 103901.

[4] D. Pan, S. Wang, B. Zhao, M. Wu, H. Zhang, Y. Wang, Z. Jiao, *Chem. Mater.* **2009**, *21*, 3136.

[5] T. Bhardwaj, A. Antic, B. Pavan, V. Barone, B. D. Fahlman, *J. Am. Chem. Soc.* **2010**, *132*, 12556.

[6] J. R. Dahn, T. Zheng, Y. H. Liu, J. S. Xue, *Science* **1995**, *270*, 590.

[7] C. H. Sun, D. J. Searles, *J. Phys. Chem. C* **2012**, *116*, 26222.

[8] Y. Li, D. Wu, Z. Zhou, C. R. Cabrera, Z. Chen, *J. Phys. Chem. Lett.* **2012**, *3*, 2221.

[9] W. W. Lei, S. Qin, D. Liu, D. Portehault, Z. W. Liu, Y. Chen, *Chem. Commun.* **2013**, *49*, 352.

[10] B. Feng, Z. J. Ding, S. Meng, Y. G. Yao, X. Y. He, P. Cheng, L. Chen, K. H. Wu, *Nano Lett.* **2012**, *12*, 3507.

[11] P. Vogt, P. De Padova, C. Quaresima, J. Avila, E. Frantzeskakis, M. C. Asensio, A. Resta, B. Ealet, G. Le Lay, *Phys. Rev. Lett.* **2012**, *108*, 155501.

[12] L. Meng, Y. Wang, L. Zhang, S. Du, R. Wu, L. Li, Y. Zhang, G. Li, H. Zhou, W. A. Hofer, H.-J. Gao, *Nano Lett.* **2013**, *13*, 685.

[13] A. Fleurence, R. Friedlein, T. Ozaki, H. Kawai, Y. Wang, Y. Yamada-Takamura, *Phys. Rev. Lett.* **2012**, *108*, 245501.

[14] C. K. Chan, R. N. Patel, M. J. O'Connell, B. A. Korgel, Y. Cui, *ACS Nano* **2010**, *4*, 1443.

[15] C. K. Chan, H. Peng, G. Liu, K. McIlwrath, X.F. Zhang, R.A. Huggins, Y. Cui,

Nat. Nanotechnol. **2008**, *3*, 31.

[16] X. H. Liu, L. Zhong, S. Huang, S. X. Mao, T. Zhu, J. Y. Huang, *ACS Nano* **2012**, *6*, 1522.

[17] G. A. Tritsaris, E. Kaxiras, S. Meng, E. Wang, *Nano Lett.* **2013**, *13*, 2258.

[18] S. M. Seyed-Talebi, I. Kazeminezhada, J. Beheshtian, *Phys. Chem. Chem. Phys.* **2015**, *17*, 29689.

[19] X. F. Fan, W. T. Zheng, J. L. Kuo, *ACS Appl. Mater. Interfaces* **2012**, *4*, 2432.

[20] C. Uthaisar, V. Barone, *Nano Lett.* **2010**, *10*, 2838.

[21] X. Wang, Y. H. Luo, T. Yan, W. Cao, M. Zhang, *Phys. Chem. Chem. Phys.* **2017**, *19*, 6563.

[22] X. Y. Shi, Z. J. Huang, M. Huttula, T. H. Li, S. Y. Li, X. Wang, Y. H. Luo, M. Zhang, W. Cao, *Crystals* **2018**, *8*, 24.

[23] X. Y. Shi, S. Posysaev, M. Huttula, V. Pankratov, J. Hoszowska, J. C. Dousse, F. Zeeshan, Y. R. Niu, A. Zakharov, T. H. Li, O. Miroshnichenko, M. Zhang, X. Wang, Z. J. Huang, S. Saukko, D. L. González, S. van Dijken, M. Alatalo, W. Cao, *Small* **2018**, *14*, 1704526.

[24] D. Chiappe, C. Grazianetti, G. Tallarida, M. Fanciulli, A. Molle, *Adv. Mater.* **2012**, *24*, 5088.

[25] H. Shu, D. Cao, P. Liang, X. Wang, X. Chen, W. Lu, *Phys. Chem. Chem. Phys.* **2014**, *16*, 304.

[26] H. Sahin, J. Sivek, S. Li, B. Partoens, F. M. Peeters, *Phys. Rev. B* **2013**, *88*, 045434.

[27] J. F. Gao, J. F. Zhang, H. S. Liu, Q. F. Zhang, J. J. Zhao, *Nanoscale* **2013**, *5*, 9785.

[28] O. Cretu, Y. -C. Lin, K. Suenaga, *Nano Lett.* **2014**, *14*, 1064.

[29] S. Najmaei, Z. Liu, W. Zhou, X. Zou, G. Shi, S. Lei, B. I. Yakobson, J. -C. Idrobo, P. M. Ajayan, J. Lou, *Nat. Mater.* **2013**, *12*, 754.

[30] O. V. Yazyev, S. G. Louie, *Phys. Rev. B* **2010**, *81*, 195420.

[31] Z. Song, V. Artyukhov, J. Wu, B. I. Yakobson, Z. Xu, *ACS Nano* **2015**, *9*, 401.

[32] Y. Liu, X. Zou, B. I. Yakobson, *ACS Nano* **2012**, *6*, 7053.

[33] A. N. Enyashin, M. Bar-Sadan, L. Houben, G. Seifert, *J. Phys. Chem. C* **2013**, *117*, 10842.

[34] H. Jamgotchain, Y. Colignon, B. Ealet, B. Parditka, J. Y. Hoarau, C. Girardeaux, B. Aufray, J. P. Bibérian, *J. Phys.: Conf. Ser.* **2014**, *491*, 012001.

[35] B. Yang, J. A. Boscoboinik, X. Yu, S. Shaikhutdinov, H. J. Freund, *Nano Lett.* **2013**, *13*, 4422.

[36] L. J. Zhou, Z. F. Hou, L. M. Wu, Y. F. Zhang, *J. Phys. Chem. C* **2014**, *118*, 28055.

[37] X. L. Sun, Z. G. Wang, Y. Q. Fu, *Carbon* **2017**, *116*, 415.

[38] B. Delley, *J. Chem. Phys.* **1990**, *92*, 508.

[39] B. Delley, *J. Chem. Phys.* **1991**, *94*, 7245.

[40] B. Delley, *Int. J. Quantum Chem.* **1998**, *69*, 423.

[41] J. P. Perdew, K. Burke, M. Ernzerhof, *Phys. Rev. Lett.* **1996**, *77*, 3865.

[42] A. Tkatchenko, M. Scheffler, *Phys. Rev. Lett.* **2009**, *102*, 073005.

[43] H. J. Monkhorst, J. D. Pack, *Phys. Rev. B* **1976**, *13*, 5188.

[44] T. A. Halgren, W. N. Lipscomb, *Chem. Phys. Lett.* **1977**, *49*, 225.

[45] G. Henkelman, H. Jonsson, *J. Chem. Phys.* **2000**, *113*, 9978.

[46] S. Li, Y. F. Wu, Y. Tu, Y. H. Wang, T. Jiang, W. Liu, Y. H. Zhao, *Sci. Rep.* **2014**, *5*, 7881.

[47] T. B. Douglas, L. F. Epstein, J. L. Dever, W. H. Howland, *J. Am. Chem. Soc.* **1955**, *77*, 2144.

[48] L. Pastewka, S. Malola, M. Moseler, P. Koskinen, *J. Power Sources* **2013**, *239*, 321.

[49] W. Cao, V. Pankratov, M. Huttula, X. Y. Shi, S. Saukko, Z. J. Huang, M. Zhang, *Mat. Chem. Phys.* **2015**, *158*, 89.

[50] M. Zhang, Z. J. Huang, X. Wang, H. Y. Zhang, T. H. Li, Z. L. Wu, Y. H. Luo, W. Cao, *Sci. Rep.* **2016**, *6*, 19504.

[51] J. Vähäkangas, P. Lantto, J. Vaara, M. Huttula, W. Cao, *Chem. Commun.* **2017**, *53*, 5428.

[52] F. Yao, F. Guenes, H. Q. Ta, S. M. Lee, S. J. Chae, K. Y. Sheem, C. S. Cojocaru, S. S. Xie, Y. H. Lee, *J. Am. Chem. Soc.* **2012**, *134*, 8646.

GRAPHICAL ABSTRACT

First-principles calculations investigated lithium adsorption and diffusion behaviors on the silicene with 5|5|8 and 4|8 grain boundaries (GBs). Besides increasing lithium adsorption energies, GBs in the 4|8 case facilitate lithium migrations on the defective plane and crossing the monolayer. Yet, silicene with GBs are predicted as a superior anode material in future lithium ion batteries with high capacity and fast charging speed.